Development of Cryogenic Filter Wheels for the HERSCHEL Photodetector Array Camera & Spectrometer (PACS)

Christian Körner*, Dirk Kampf* ,Albrecht Poglitsch**, Josef Schubert**, U. Ruppert+ and M. Schoele+

Abstract

This paper describes the two PACS Filter Wheels that are direct-drive rotational mechanisms operated at a temperature below 5K inside the PACS focal plane unit of the Herschel Satellite. The purpose of the mechanisms is to switch between filters. The rotation axis is pivoted to the support structure via a slightly preloaded pair of ball bearings and driven by a Cryotorquer [1]. Position sensing is realized by a pair of Hall effect sensors. Powerless positioning at the filter positions is achieved by a magnetic ratchet system. The key technologies are the Cryotorquer design and the magnetic ratchet design in the low temperature range. Furthermore, we will report on lessons learned during the development and qualification of the mechanism and the paint.

Introduction and Requirements

HERSCHEL is an ESA Cornerstone mission to study the origin and evolution of stars and galaxies. Three cryogenic instruments are accommodated in the focal plane of the Herschel telescope: HIFI, SPIRE and PACS. The giant infrared space observatory was launched on 14 May 2009 on an Ariane 5 and successfully operated in an orbit around L2 until end of April 2013, when the cryostat ran out of liquid helium coolant. The PACS instrument operates either as an imaging photometer or an integral field spectrometer over the spectral band from 57 to 210 µm. Inside the PACS instrument, several mechanisms are accommodated: a Chopper to switch between the sky field of view and internal calibration sources, a Grating Drive to scan through the spectral band, and two Filter Wheels to select spectral bands for the observation which are subject of this paper. The main requirements for the Filter Wheels are listed in Table 1.

Table 1: Filter Wheel Main Requirements

	Requirement
Mass	Max. 1000 g
Quasi-static load	25g
No of revolutions incl. ground test and ECSS margins (qualification @ LHe)	40000
Operational temperature range	1K…350K
Amount of Filters	2 (initially 4)
Switching time (180°)	5 sec
Powerless position preservation	±30 arcmin (0.5 Ncm @3°)
Stray light reduction (on instrument level)	10^8
Power dissipation 4K level:	50 mWs per switching

* Kayser-Threde GmbH, Munich, Germany

** Max Plank Institut für extraterrestrische Physik, Garching, Germany

+ Freie Universitat Berlin, Berlin, Germany

Accommodation

In order to reduce the amount of sliding, rolling or flexing parts and due to mechanical and optical envelope reasons, a rotating system with a rotating cone supporting the filters was selected. The bearings are accommodated around the center of gravity of the rotating mass. The rotor of the Filter Wheel drive acts as a counterweight to the mass of the Filter Wheel and filters. To keep the wheel assembly compact, the position sensors and the magnetic ratchet system are accommodated in one plane with the lower bearing. The Filter Wheel drive, which was provided by FU Berlin, consists of a two-part rotor equipped with two sets of permanent magnets on both sides of the coils and a stator that is locatred between the magnets of the rotor and carries the windings (see Figure 6).

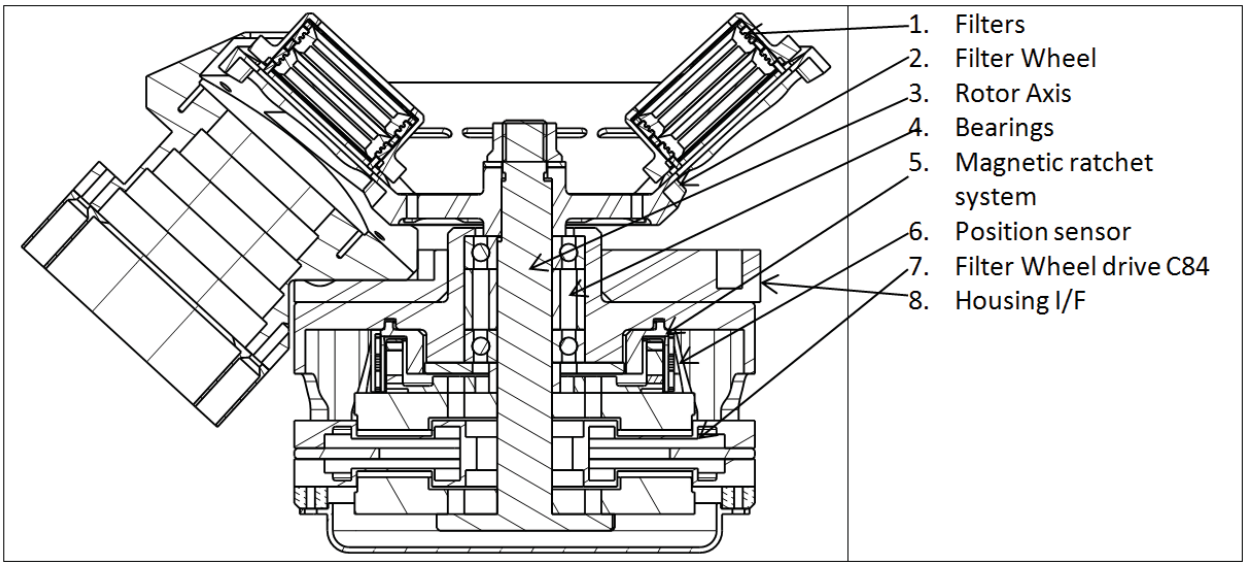

Figure 1. Filter wheel configuration

Bearing system

The bearing is located in between the filters and the rotor of the motor. This allows a counterweighted configuration of the movable parts. The Filter Wheel with all the rotating parts (Cryotorquer Rotor, Wheel cone, Filters Axis…) has a mass of <600 g. The maximum quasi-static acceleration (derived from the Instrument FEM) is 26 g. To avoid gapping of the bearing, a preload of 126 N would have to be applied. But since the wheel shall be optimized to run with low power dissipation (50 mWs per switching), the preload is reduced to a minimum and the higher amplification and friction (during vibration) in the bearing is taken into account by a higher load capability. The selected bearing configuration is an O-configuration of two GRW SS6900 Z C10/15 GPR-1 J ball bearings.

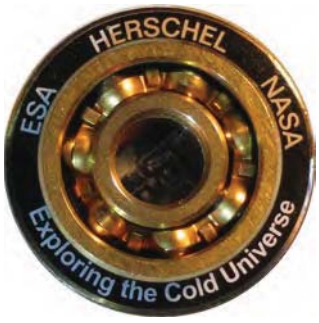

Figure 2. Gold-lubricated GRW SS6900 Z C10/15 GPR-1 J Ball bearing

Each of these bearings has 1130-N static load capability, which is assumed to be sufficient taking into account that the bearing adds damping due to friction (2% damping assumed). The low temperature forces the choice of a solid film lubrication. In order to avoid sensitivity to moisture, gold is selected. Gold lubrication shows a temperature and humidity independent behavior and is acceptable for this application due to the low number of revolutions.

Axial fit: To keep the preload constant over a temperature range of 300K, the bearings and the distance rings (which adjust the preload) have to be made out of the same material (or at least material with the same CTE). These distance rings are shimmed with precision shims to adjust a friction torque below 5 mN-m.

Radial fit: The housing material and all other parts of the PACS structure and mirrors are made of aluminum AA6061 in order to have an instrument that can be aligned at 293K and operated at 4K. The fitting of the bearing diameter therefore has to take into account the relative shrinkage between stainless steel and aluminum in the temperature range between 290K and 4K. The shrinkage can be approximated as a 5th order polynomial equation.

Polynomal eqotation for the temerpaturedependent CTE (NIST) for Aluminium and Steel

$a_{Al} := -4.1272 \cdot 10^{-2}$ $b_{Al} := -3.064 \cdot 10^{-1}$ $c_{Al} := 8.796 \cdot 10^{-3}$ $d_{Al} := -1.0055 \cdot 10^{-5}$ $T_{min} := 4$

$L_{293} := 22$ Bearing outer Diameter @ 293K

$$LAl_T := \left(a_{Al} + b_{Al} \cdot T_{min} + c_{Al} \cdot T_{min}^{2} + d_{Al} \cdot T_{min}^{3}\right) \cdot 10^{-5} \cdot L_{293} + L_{293}$$

$LAl_T = 21.909$ Housing Diameter @ 4K

$a_{SS} := -2.9546 \cdot 10^{-2}$ $b_{SS} := -4.0518 \cdot 10^{-1}$ $c_{SS} := 8.796 \cdot 10^{-3}$ $d_{SS} := -1.0055 \cdot 10^{-5}$

$e_{SS} := 1.8780 \cdot 10^{-8}$

$$LSS_T := \left(a_{SS} + b_{SS} \cdot T_{min} + c_{SS} \cdot T_{min}^{2} + d_{SS} \cdot T_{min}^{3} + e_{SS} \cdot T_{min}^{4}\right) \cdot 10^{-5} \cdot L_{293} + L_{293}$$

$LSS_T = 21.935$ Bearing Diameter @ 4K

$\Delta l := LSS_T - LAl_T$ $\Delta l = 0.026$ Differential shrinkage 293K...4K

Therefore, the fitting diameter of the ball bearing housing is 26 µm larger in order to compensate for the shrinkage.

Position Device

To ensure powerless positioning at the filter positions, the Filter Wheel is equipped with a magnetic position device. The setup of the magnetic position device (90°) is sketched in Figure 3.

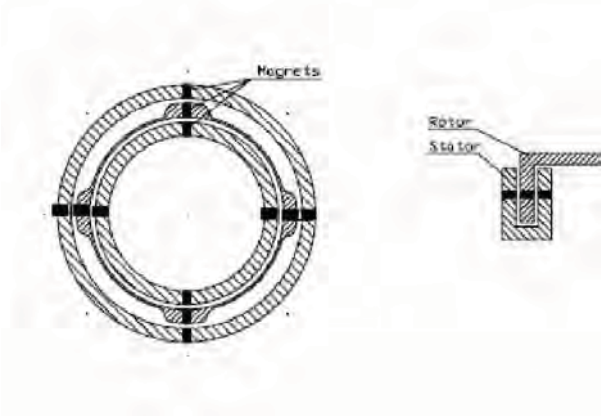

Figure3. Locking system schematic

By design, the Filter Wheel is balanced. Therefore, under gravity there are only extremely low torques (<1 mN-m) due to backdriving moments due to eccentricity or residual magnetic fields. In space, there will be almost no backdriving moment at all. The bearing friction cannot be assumed as a powerless positioning device. Therefore, a magnetic ratchet system was implemented. The torque of the actuator is linear to the current but the Ohmic power consumption goes with the second power of the current. Therefore, the ratchet torque is set to a low level (10 mN-m which is roughly twice the max friction). This value adds the functionality of automatic centering (without ECSS margins). The implemented solution is a set of 3 SmCo magnets in series where the middle one is mounted to the rotor. This configuration is repeated in a 90° pattern. To achieve the requested torque, SmCo magnets with a diameter of 1.5 mm and a length of 3 mm were selected.

Position Sensor

In order to keep the dissipation in the system low and to increase reliability, the position sensor is implemented using contactless technology. The position sensing is performed by Hall effect sensors that detect the magnetic field of magnets mounted on the rotor.

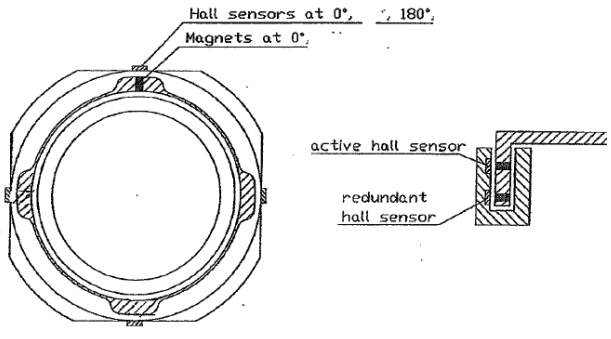

Figure 4. Decoder system schematic

The selection of the sensor is based on the following parameters: operating temperature range, low dissipation, and linearity. To work at the temperature range of 4.2K the Infineon ion-implanted GaAs hall generator KSY 10 was selected. The hall current was set from 7 mA to 0.75 mA, which reduces the hall voltage from 200 mV to ~20 mV. This is sufficient to detect the position with an accuracy better 10 arcmin

at the instrument level but at the same time reduces the power dissipation by a factor of 10. The dissipated power at 4.2K for a 180° switch is then:

0.85 mW * 2 (positions nominal)*5 sec (switching time)= 8.5 mWs.

For this application, the SmCo magnets from the position device (dia.1.5 mm*3 mm) are reused. Note: For the actual 90° ratchet system (double magnets) the torque has to be doubled.

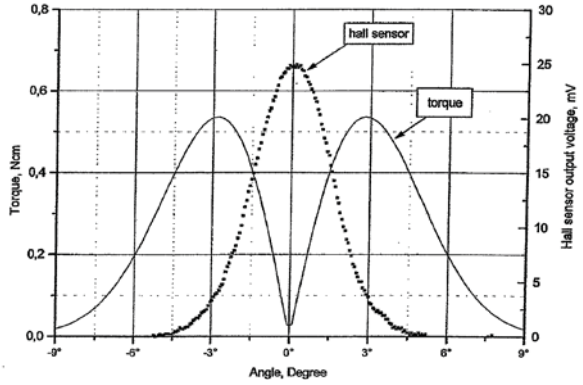

Figure 5. Absolute value of the Hall sensor signal and the restoring torque for a 180° magnetic ratchet system

Actuator

In this application, the driving parameter for the sizing of the motor is not the motorization (as usual in space mechanisms), but power/heat dissipation since the lifetime of the mission is dependent on the dissipation inside the cryostat. In general, dissipation is minimized when the efficiency of the motor is high, friction is minimized, and the motor inertia and the actuated inertia are approximately equal. The Filter Wheel rotating parts have an inertia of ~0.1 g-m²; this fits into an already existing Cryotorquer developed by the FU Berlin (C 84) ** with an inertia of 0.12 g-m². This Cryotorquer has also a high efficiency for slow rotating torque applications at low temperature. In addition, this Cryotorquer has heritage from several low temperature space projects. Therefore, this Cryotorquer was selected.

The pancake-shaped electronically commutated torque motor C84 developed by the FU Berlin is described in Figure 6.

The rotor consists of a package of alternating SmCo magnets on both sides of the coils (stator) that allows a comparable high air gap (0.5 mm) without decreasing performance. The magnetic loops are closed by means of the yoke rings made of good permeability material for low temperatures. The stator is composed of two redundant coil packages and each consists of one set of coils for phase 1 and a second set for phase 2. In normal operation, the two coil sets for each phase are interconnected. The current for each phase is supplied by the corresponding power source of the electronic control unit.

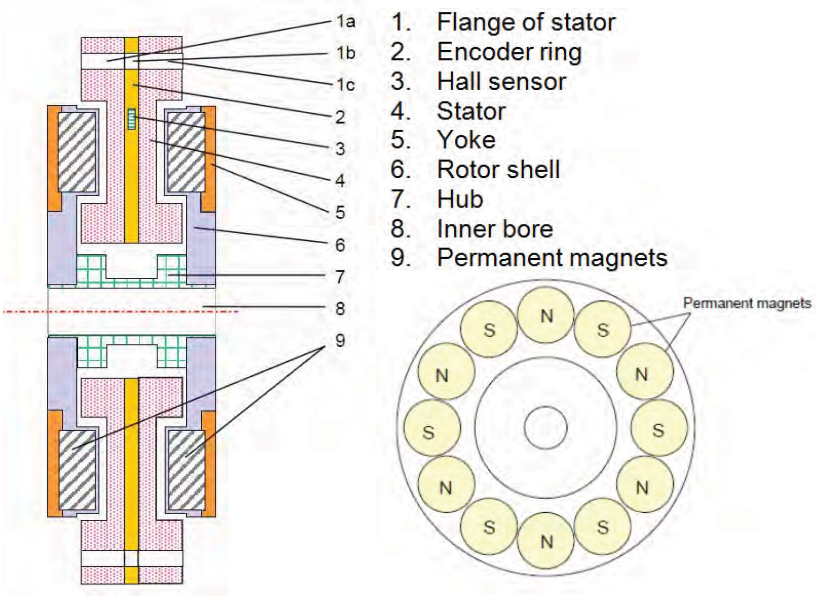

Figure 6. Schematic cross section of the Cryotorquer C 84 developed by FU Berlin

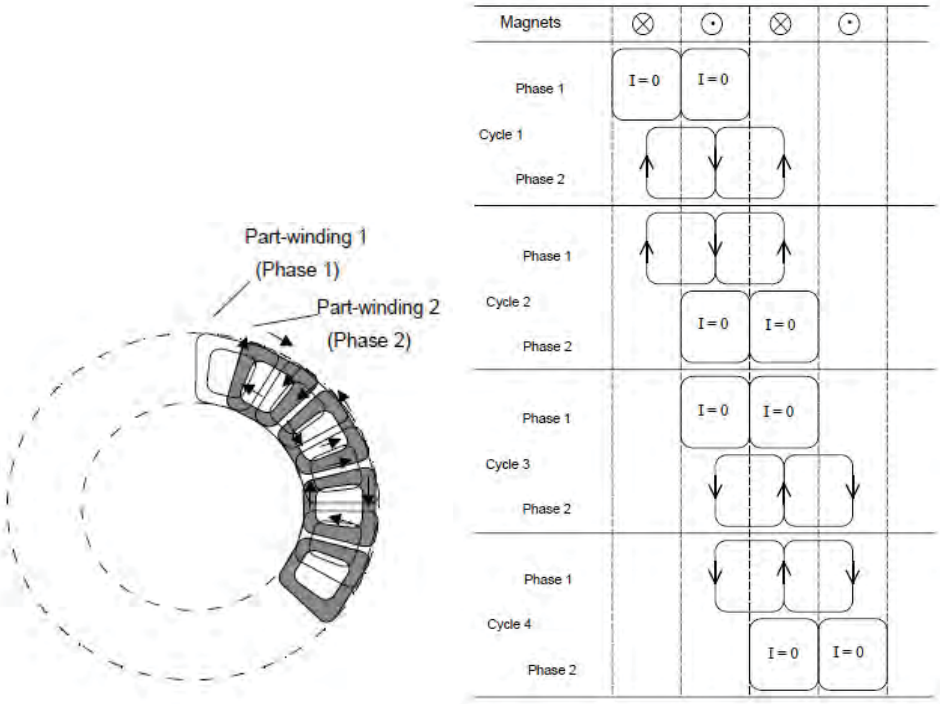

Figure 7. Position of the coil-sets of the two phase indicating the 15° angle shift of the two sets and an example for the current vectors of the two phases.

The torque capability of the motor at 250 mA is 142 N-mm. The maximum torque needed is 5 mN-m for the friction and 10 mN-m for the positioning device.

Worst case dissipation for 180° movement

$Current_{max} := 27mA$ $T_{switch} := 5s$

$Ressistance_{4k} := 3.6\Omega$ $P_{max} := (Current_{max})^2 \cdot Ressistance_{4k}$

$P_{max} = 2.6 \times 10^{-3} \cdot W$ $k_m := 0.3 \frac{N \cdot m}{\sqrt{W}}$

$Torque := k_m \cdot \sqrt{P_{max}}$ $Torque = 0.015 \cdot N \cdot m$

$Dis := P_{max} \cdot T_{switch}$ $Dis = 13 mW \cdot s$

Development of the Coating

In order to achieve the demanding stray light reduction requirements, a new coating had to be developed since there is no coating commercially available that reduces the stray light at a wavelength of 57 to 200 µm significantly. Therefore, KT has developed a coating (KT-72) which is indeed highly effective with respect to stray light reduction but at the same time bears some risks for the mechanisms.

In order to have reasonable stray light reduction, the effect of black paint in the optical path in the coating has to be of the order of magnitude of the wavelength or higher. The thickness of the paint inside the PACS instrument was therefore set in the range of 400 to 500 µm, which is far away from the thickness of standard paints. In addition, the coating includes glass beads in order to change the direction of the light path into the plane of the coating.

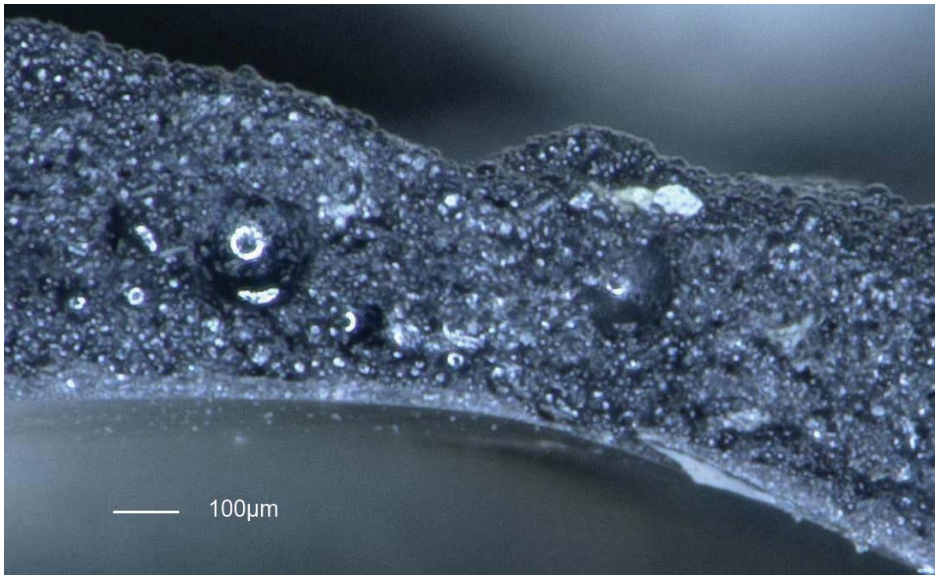

Figure 8. Cut through a KT-72 sample.

During the development of the coating, two effects drove the development, the delta CTE of the materials and the aerodynamic configuration.

The delta CTE of Paint (~40e-6) / Glass (6-) and Aluminum (14) (Housing) and a temperature gradient of 400K (bake out) to 4K leads to high stresses in the paint and between the coating and the base material,

which is at the limit of feasibility. Therefore, the connection between the different layers had to be optimized. One major parameter is time. The time-dependent oxidation and the contamination between the layers avoid a perfect adhesion. ALODINE is known as a very good surface to apply coatings. But for our coating, this turned out to be only sufficient when the coating was applied within 48 hours after ALODINE application. After this period, a reactivation of the surface became necessary.

First tests were made with flat samples. But this turned out to be not sufficient since the aerodynamic configuration of the parts have an influence to the distribution between large and heavy particles and paint µ-particles. Therefore the result varies with the geometrical setup. The complex setup of the instrument did not allow a flat configuration of coating application. Therefore, KT did not change the source of the contamination but the effect.

The surfaces that had a “bad shape” and contained loose particles were “brushed” with a conventional electrical toothbrush. All parts were cleaned with a clean room vacuum cleaner.

Test Results

The following development tests were performed by the FU Berlin:
- Vibration tests at 4.2K (sine search, sine, random)
- Functional and performance tests at 4.2K after vibration tests

For the tests at 4.2K, the Filter Wheel was placed in a sealed container.

Figure 9. PACS FW in the sealed vibration adapter

In Figure 10, the test results before and after the vibration tests are shown.

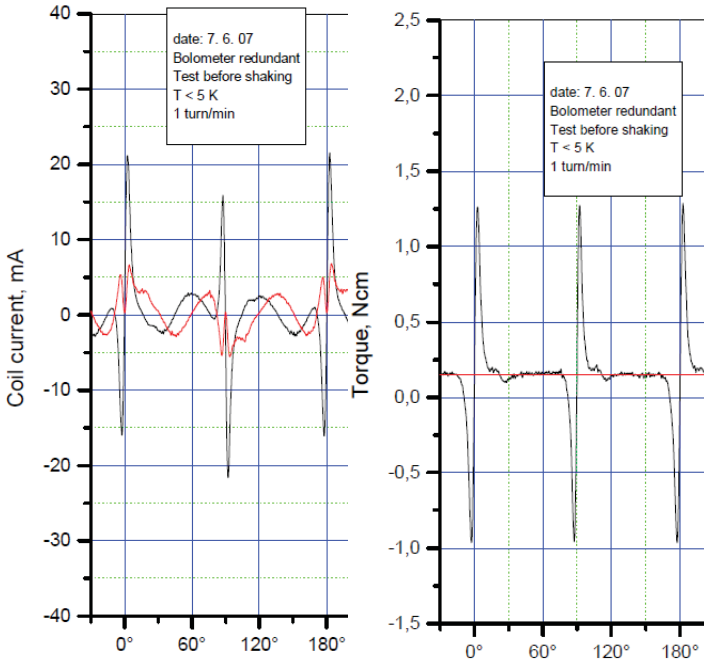

Figure 10. Current (winding 1+2) and torque of the two redundant coils before vibration

The functional test of the Filter Wheel shows very smooth rotation with 1.8 mN-m average torque. The high spikes (±12 mN-m) are due to the magnetic ratchet system

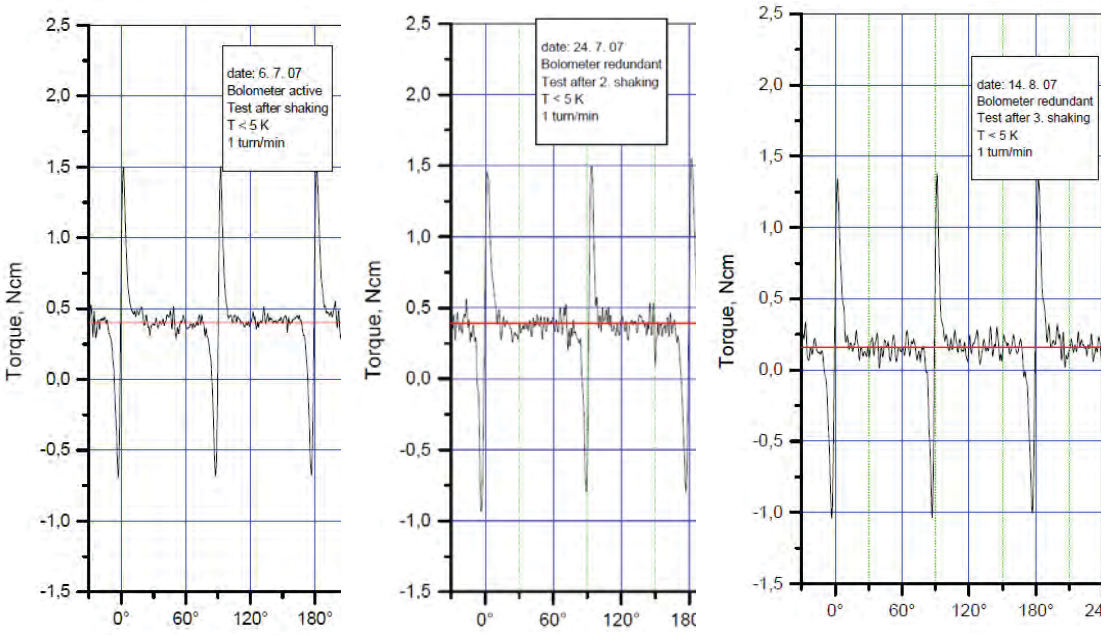

Figure 11. Torque after vibration tests

The first graph in Figure 11 shows the torque after the 0.5g sine search between 5 and 2000 Hz at 4.2K. The torque increased to 4 mN-m with a ripple of 1 mN-m. The second graph in Figure 11 shows the torque after the full sine vibration between 5 and 100 Hz with 19.8g max acceleration. The torque is

slightly decreased to 3.8 mN-m with a ripple of 1 mN-m. Torque after random vibration with 7.3g RMS → lower average torque but ~1.5 mN-m ripple.

The lifetime test at 4K (40000 start stop cycles) showed no increase in torque.

A failure of the Filter Wheel mechanism occurred during ground-testing of the flight spare instrument. While this failure (clamping) could be explained by exceeded manufacturing tolerances and recovered by shimming, it was nevertheless decided at instrument level to increase the motor current to gain a higher safety margin for the on-orbit operation.

Flight Data

Over the whole mission (4 years in orbit and 2 years on ground) no failure occurred. The temperature over the whole in-orbit lifetime was stable at 2.92K. The wheel was driven with constant current sine of 70 mA which generates a torque of 56 mN-m for the nominal windings, a value which is considered as necessary and sufficient to overcome the bearing friction.

The photometer Filter Wheel performed ~6000 rotations the spectrometer Filter Wheel ~3000. The flight data we received for the evaluation are the Spectrometer Filter Wheel data from BOL (2009) and EOL (20013), which are shown hereafter.

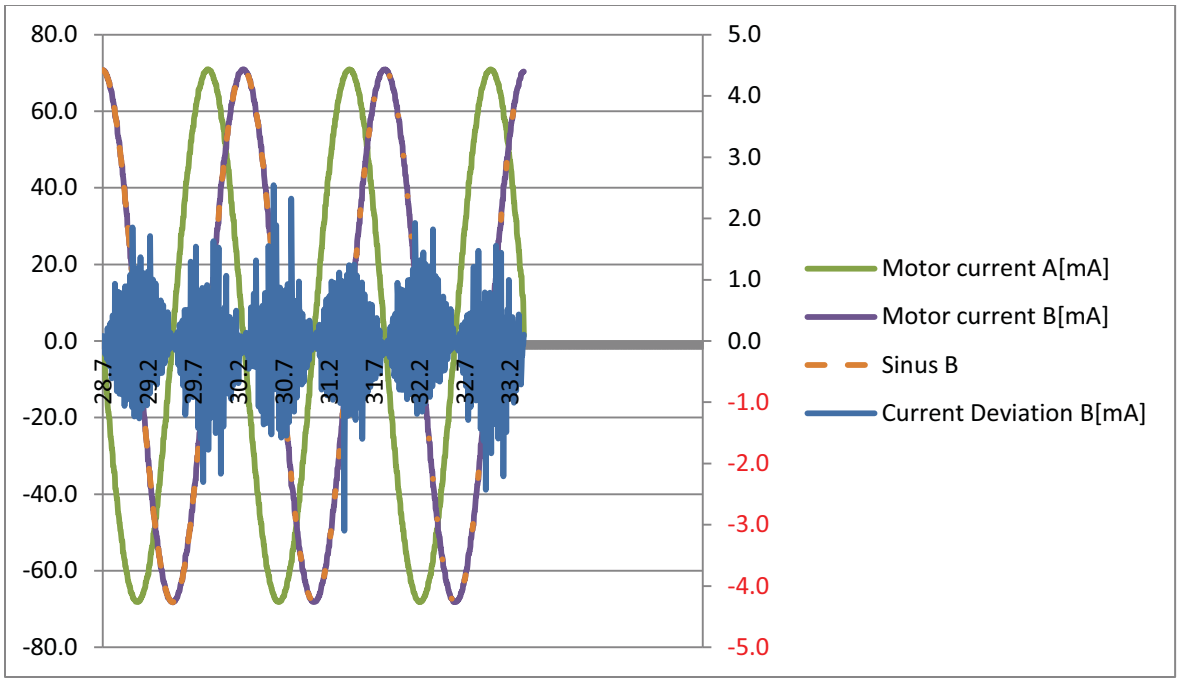

Figure 12. Current and ripple of the nominal coils during flight

The magnetic field readout of the motor hall sensors shows the smooth movement with no significant change between BOL and EOL. Since the Filter Wheels operated inconspicuously there are only very few high-speed data records from the operation of the wheels.

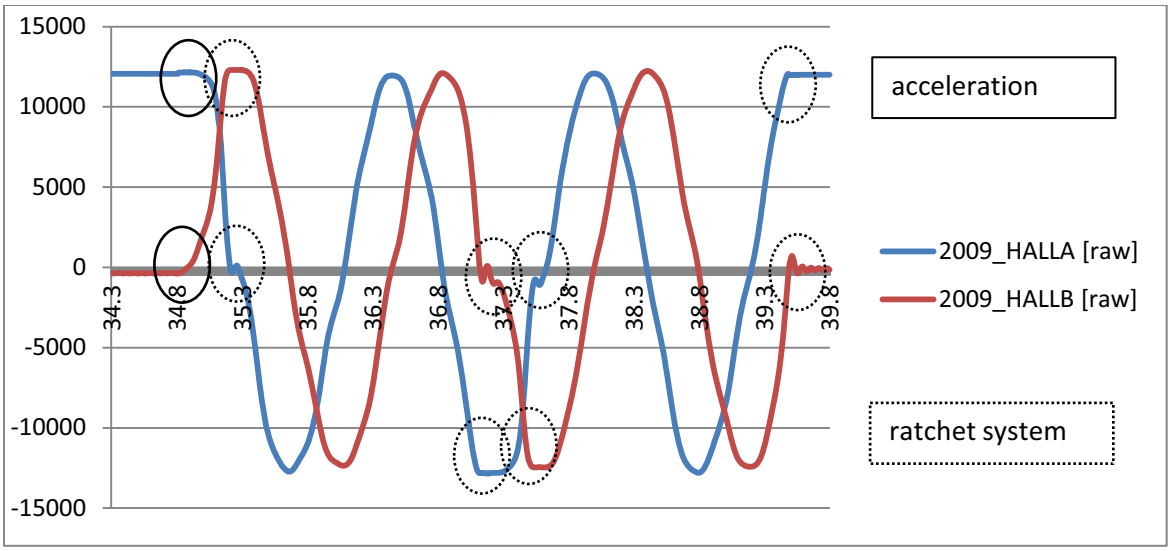

Figure 13. Signal of motor Hall sensors during commissioning

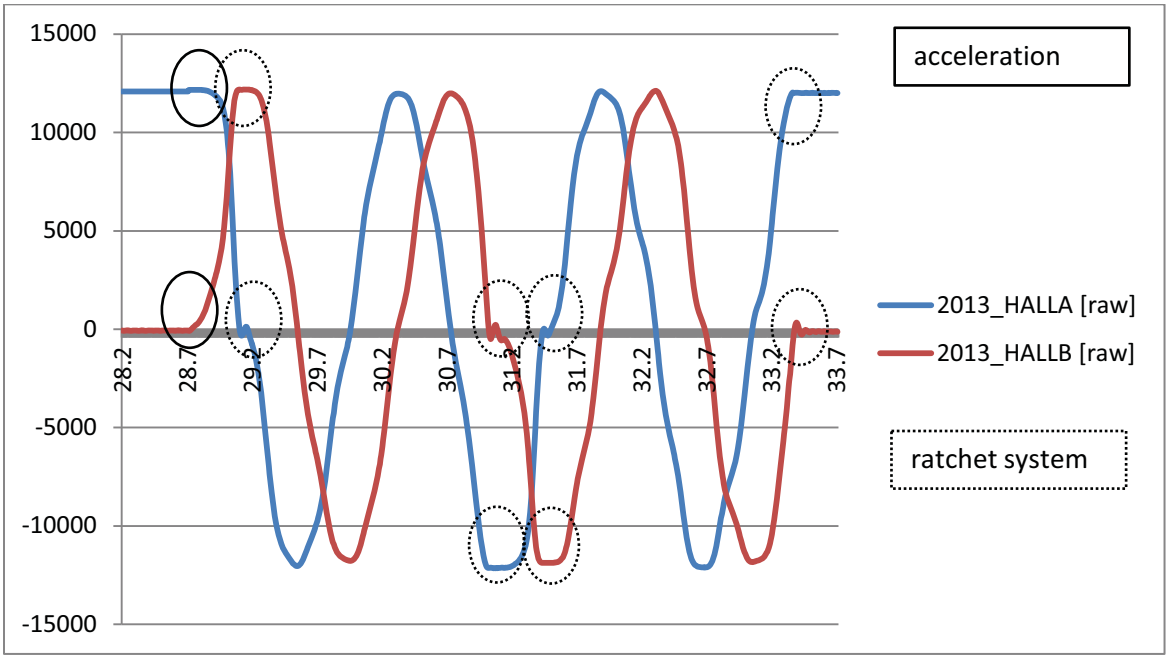

Figure 14. Signal of motor Hall sensors at end of life

Conclusions and Lessons Learned

The development of the PACS Filter Wheels was successful and the two flight models performed well in the Herschel program. The usage of an already existing and proven cryotorquer eased the development. Also the contactless ratchet system and the contactless sensors were very predictable and reliable. Only the bearing showed some degradation during the vibration tests. The torque ripple increased to 1.5 mN-m and the overall torque showed some unpredictable variation after the vibration tests. In order to avoid such a variation, the complete bearing should be suspended in a setup where all CTE's are

matched to the bearing CTE. This homogeneous thermal shrinking setup was then isostatically mounted against the housing.

In addition, a deviation from the specified manufacturing tolerances in the flight spare model has led to a clamping in the flight spare mechanism that could be recovered by additional shimming.

The development of the paint was the highest risk for the function of the Filter Wheels since one of the 100-µm glass beads could destroy a ball bearing and thus stop the Filter Wheel. The huge effort that was put into the development of the coating has paid off.

References

1. M. Schoele, U. Ruppert,
   “CRYOGENIC MOTORS FOR HERSCHEL/PACS AND JAMES WEBB/MIRI AND NIRSPEC"
   FUB (Freie Universität Berlin), Department of Physics, Low Temperature Laboratory, Arnimallee 14, 14195 Berlin, Germany